JOURNAL OF APPLIED ELECTROCHEMISTRY **16** (1986) 663–668

High temperature-type proton conductive solid oxide fuel cells using various fuels

H. IWAHARA, H. UCHIDA, S. TANAKA

Department of Environmental Chemistry and Technology, Faculty of Engineering, Tottori University, Minami 4-101, Koyama-cho, Tottori 680, Japan

Received 24 July 1985; revised 1 October 1985

Using a high temperature-type proton conductive solid electrolyte based on $SrCeO_3$, the performances of various types of fuel cells were studied at 800 to 1000° C. Ethane, carbon monoxide and ethanol were used as the fuel. In the ethane–air fuel cell, the simultaneous generation of electricity and ethylene could be carried out without oxidizing ethylene into carbon dioxide. These cells worked stably and the major limitation of the cell system was the resistance of the solid electrolyte.

1. Introduction

High temperature solid electrolyte fuel cells have inherent advantages over other fuel cell types. Due to the high operating temperature, high current and power densities are achieved without the use of noble metal catalysts. Also, this type of cell produces high quality waste heat. Many investigators have studied high temperature fuel cells using oxide ion conductive solid electrolytes such as stabilized zirconias [1–15] and other oxides [16, 17]. Proton conductive solids are also favourable materials as the solid electrolytes for such fuel cells.

Several years ago, we discovered high temperature-type proton conductive solid electrolytes based on $SrCeO_3$ and fabricated a fuel cell using these as a diaphragm and porous platinum as an electrode material [18–21]. The cell worked stably at 800 to 1000° C. It was confirmed that, on discharging the cell, water vapour was produced at the air electrode at a rate corresponding to Faraday's law. This fact indicates that the charge carrier in this electrolyte is a proton and not the oxide ion. Fig. 1 shows the difference between the proton conductor and oxide ion conductor in such fuel cells. The polarization phenomena of platinum electrodes in high temperature-type proton conductor fuel cells were also studied [22]. Using the same electrolyte, we have demonstrated proton conduction in studies on a steam electrolyser for hydrogen production [18–20], a steam concentration cell [18, 23, 24] and a hydrogen concentration cell [25].

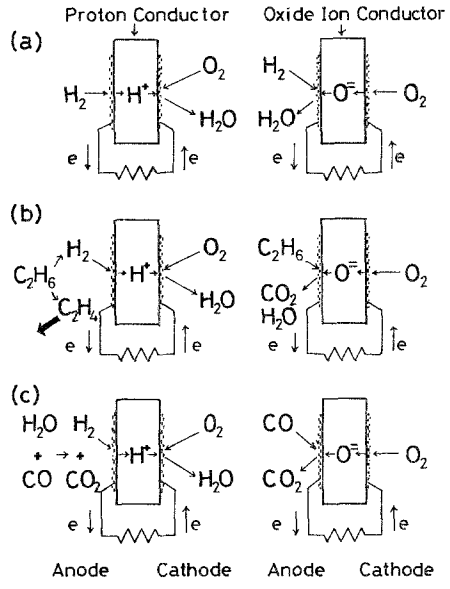

Fig. 1. Schematic illustrations of the operation principles of the solid electrolyte fuel cells. Fuel gas: (a) hydrogen, (b) ethane, (c) carbon monoxide.

Another advantage for the high temperature solid electrolyte fuel cell is the wide choice of fuels. The fuel reformer required in both the alkaline and the phosphoric acid fuel cell system is not needed in this kind of cell. In oxide ion conductor cells, not only hydrogen but also

0021-891X/86 $03.00 + .12

carbon monoxide [2, 7], ammonia [8], hydrocarbons [12, 16] and solid carbon [17] could be used as the fuel.

For proton conductor fuel cells, various fuels are also possible. Since only the hydrogen gas, which is produced by the 'internal reforming' of fuels, takes part in the anodic reaction ($H_2 \rightarrow 2H^+ + 2e$) in this case, the residual fraction of the reformed products can be obtained from the anode compartment, whereas in the oxide ion conductor cell, fuels are oxidized to H_2O or CO_2 at the fuel electrode. For example, when ethane is supplied to the proton conductor cell, the following pyrolysis reaction occurs in the anode compartment

$$C_2H_6 \longrightarrow C_2H_4 + H_2 \qquad (1)$$

While hydrogen is consumed by the cell reaction, ethylene is not oxidized to CO_2 in this cell (Fig. 1b). Therefore, this cell device can generate both electric power and ethylene by consuming ethane as a fuel. Since the pyrolysis of hydrocarbons is an important route to the production of ethylene in the petrochemical industry, this cell may be suitable as an on-site electric generator for ethylene plants.

In this study the performances of the hydrocarbon (ethane) fuel cell is examined using a high temperature-type proton conductive solid electrolyte based on $SrCeO_3$. Some attempts to use other fuels ($CO + H_2O$, C_2H_5OH) for this cell are also described.

2. Experimental details

The proton conductive solid electrolyte used in this study was the ceramic $SrCe_{0.95}Yb_{0.05}O_{3-\alpha}$, where α is the number of oxygen deficiencies per perovskite-type unit cell. The preparation of the ceramic was similar to that in the previous study [18, 22]. The sinters obtained were sliced into thin discs (thickness: about 0.5 mm, diameter: 12 mm) to provide test specimens.

The construction of the solid electrolyte fuel cell was the same as in references [20, 21]. Porous platinum electrodes were attached to both faces of the electrolyte disc (projected area: 0.5 cm^2). Porous nickel was also used as the fuel electrode [21]. A platinum wire was wound around the side of the electrolyte disc as the reference electrode. The electrode compartments were separated by the ceramic electrolyte and each electrode compartment was sealed by a glass ring gasket. The cell was situated in an electric furnace.

The fuel gases used in this study were C_2H_6 (Seitetsu Kagaku, 99.0%), CO (Seitetsu Kagaku, 99.0%) and C_2H_5OH vapour. Ethane and carbon monoxide were used from the commercial cylinder without purification. The partial pressure of water vapour, P_{H_2O}, in the gases was controlled by saturating with water vapour at a given temperature. In order to supply C_2H_5OH vapour in the cell, argon gas was saturated with aqueous ethanol (1 : 1) at a given temperature. On the cathode side, air was used in the wet state. The total pressure of both electrode gases was 1 atm ($= 1.013 \times 10^5$ Pa) in all cases.

The gas analysis was carried out by a gas chromatograph (Shimazu, Model GC-3BT, carrier gas: argon). As the column packing, Porapak Q (CO_2, C_2–C_3 hydrocarbons) and molecular sieve 5A (H_2, O_2, N_2, CH_4, CO) were used. A thermal conductivity detector and an automatic integrator (SIC, Model 5000E) were employed.

Polarization characteristics of the electrodes were studied by a current interruption method [22].

3. Results and discussion

3.1. *Ethane fuel cell*

Using $SrCe_{0.95}Yb_{0.05}O_{3-\alpha}$ as the solid electrolyte and porous platinum as the electrode material, the ethane–air fuel cell was constructed. Typical cell performances are shown in Fig. 2. The cell worked as stably as the hydrogen–air fuel cell [18–22]. The e.m.f.s were 930 mV at 800° C and 958 mV at 900° C, respectively. From this e.m.f. value, the partial pressure of hydrogen at the anode can be estimated to be 0.125 atm at 800° C and 0.385 atm at 900° C, assuming that the proton transport number is 0.95 [18]. A steady and stable current could be drawn and the relation between the terminal voltage and the current density was linear.

Fig. 3 shows the polarization characteristics of the fuel and air electrodes. Since the ohmic

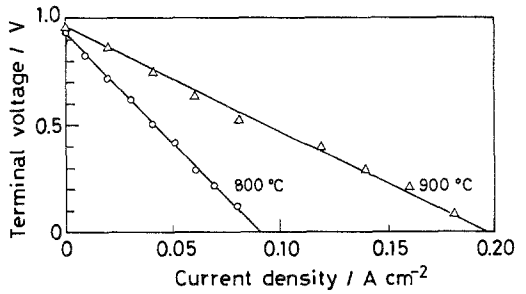

Fig. 2. Performance of the C_2H_6–air fuel cell; C_2H_6, Pt|$SrCe_{0.95}Yb_{0.05}O_{3-\alpha}$|Pt, air ($P_{H_2O}$ is 33.7–34.7 torr in both gases).

drop was large compared to the residual voltage drop, the major limitation of this fuel cell can be regarded as the resistance of the solid electrolyte as observed in our previous cells [18–22]. The potential of the fuel electrode, corrected for ohmic loss, exhibits an almost constant value against the reference electrode over the whole range of current density examined (< 0.2 A cm^{-2}). Therefore, the anodic reaction ($H_2 \rightarrow 2H^+ + 2e$) can be considered to occur reversibly even in the atmosphere with a relatively low concentration of hydrogen. Similarly to the hydrogen–air fuel cell, the polarization at the cathode ($2H^+ + \frac{1}{2}O_2 + 2e \rightarrow H_2O$) could not be neglected in this cell. The polarization resistance for the cathode was somewhat higher than that in the previous cell [22]. However, such a difference may be due to the difference in the surface state of the porous electrodes, and the rate-determining step of the cell reaction is probably the mass transport of oxygen atoms [22].

When dry argon was supplied to the cathode compartment instead of air and direct current

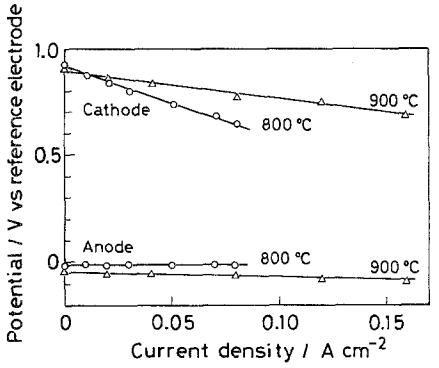

Fig. 3. Polarization characteristics of the electrodes (the cell is the same as in Fig. 2).

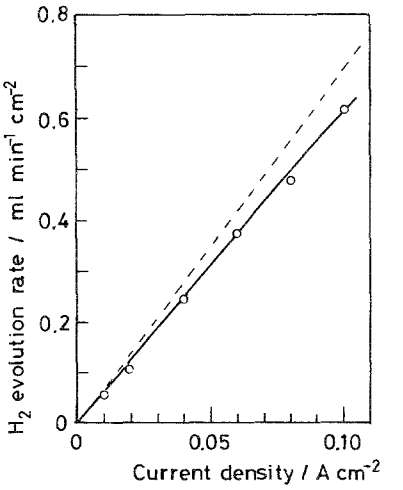

Fig. 4. Electrochemical extraction of hydrogen at 800° C in the cell; C_2H_6, Pt|$SrCe_{0.95}Yb_{0.05}O_{3-\alpha}$|Pt, Ar ($P_{H_2O}$ in C_2H_6 is 28.3 torr) (broken line shows the theoretical rate).

was passed through the electrolyte, the evolution of hydrogen gas was detected at the cathode by gas chromatography. Fig. 4 shows the hydrogen evolution rate as a function of current density. The evolution rate was close to the theoretical rate calculated from Faraday's law. This indicates that the charge carrier in this ceramic electrolyte is a proton even in this atmosphere and that this cell device acts as the electrochemical hydrogen extractor.

In place of expensive platinum, porous nickel could be used as the hydrogen electrode and exhibited little polarization [21]. Porous nickel was attached to the electrolyte and the ethane–air fuel cell was constructed. The cell with the nickel anode worked stably as shown in Fig. 5. Fig. 6 shows the polarization characteristics of the electrodes. The nickel anode showed a

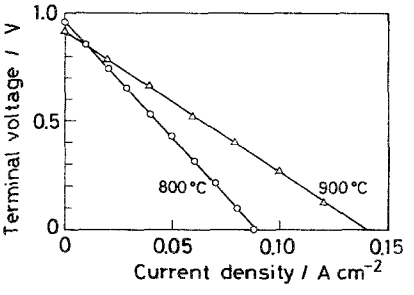

Fig. 5. Performance of the fuel cell with nickel anode; C_2H_6, Ni|$SrCe_{0.95}Yb_{0.05}O_{3-\alpha}$|Pt, air ($P_{H_2O}$ is 31.8 torr in both gases).

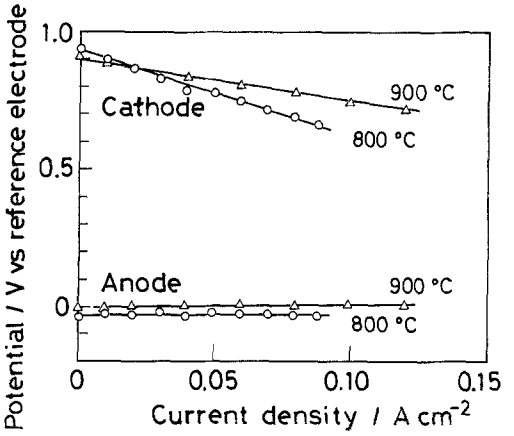

Fig. 6. Polarization characteristics of the electrodes in the same cell as in Fig. 5.

negligibly small anodic polarization at the current densities examined although the contact resistance must be improved.

Exhaust gas from the anode compartment was analysed by gas chromatography. Typical results are shown in Table 1. The exhaust gas contained H_2, C_2H_4, CH_4, C_2H_6 and trace amounts of CO, CO_2, C_3H_8 and C_3H_6 (the origin of C_3H_8 and C_3H_6 was the impurity in the ethane gas used). The deposition of solid carbon (brown coloured char) was also observed at the outlet of the anode. This indicates that various pyrolysis reactions occur besides Equation 1 [26–28].

$$C_2H_6 \longrightarrow \tfrac{1}{2}C_2H_4 + CH_4 \qquad (2)$$

$$C_2H_6 \longrightarrow 2C + 3H_2 \qquad (3)$$

$$C_2H_4 \longrightarrow 2C + 2H_2 \qquad (4)$$

Table 1. Composition of the exhaust gas from C_2H_6–air fuel cell at open circuit. C_2H_6 feed rate = 50 cm^3 min^{-1}, P_{H_2O} = 31.8 torr

Cell Temp. (° C)	*Electrode*	*Composition (vol %)*			
		H_2	*C_2H_4*	*C_2H_6*	*CH_4*
800	Platinum	18.3	11.7	68.4	1.2
	Nickel	13.6	8.7	76.1	0.3
900	Platinum	34.7	30.3	25.7	8.8
	Nickel	34.9	35.0	26.9	3.2

* Trace: CO_2, CO.

The composition of the gas depended on the cell temperature, the flow rate of gas, the amount of water vapour in the C_2H_6 and the electrode material. The content of H_2 and C_2H_4 increased with increasing temperature, since ethane is easily pyrolysed at higher temperature (free energy, ΔG for Equation 1 is $-0.27\,kJ\,mol^{-1}$ at 800° C and $-1.04\,kJ\,mol^{-1}$ at 900° C) [26–28]. The analysed value for hydrogen agreed with the hydrogen partial pressure calculated from the e.m.f. as described above.

The effect of the discharge current on the composition of the exhaust gas is not so clear since the electrode area is small and the current is not so high. However, it was confirmed, as expected from Fig. 1b, that CO_2 was not formed at the anode on discharging the cell. Recently, Stoukides and Vayenas [29] have reported that the catalytic rate of propylene epoxidation on a porous silver electrode increased significantly when oxide ions were pumped electrochemically to the electrode on yttria stabilized zirconia electrolyte. On the other hand, since hydrogen is electrochemically pumped out from the anode compartment, such electrocatalytic rate enhancement for various organic synthesis can be expected on discharging our proton conductor fuel cell. Such studies are in progress.

3.2. *Some other fuel cells*

Some other fuels were also used in the proton conductor cell. Firstly, carbon monoxide saturated with water vapour at room temperature was used. When wet CO is introduced to the cell, hydrogen should be produced by water–gas-shift reaction

$$CO + H_2O \overset{K}{\rightleftharpoons} H_2 + CO_2 \qquad (5)$$

The equilibrium is easily established at the operating temperature of the cell (> 800° C). Judging from the equilibrium constant K [30], almost all H_2O added to CO can be converted to H_2 and CO_2 in this condition. Hydrogen thus produced would take part in the anodic reaction of the cell. On introducing wet CO into the anode compartment, the cell exhibited an e.m.f. close to the theoretical e.m.f. and the ionic transport number was above 0.95 at 800 to 1000° C. This cell showed stable discharge characteristics above

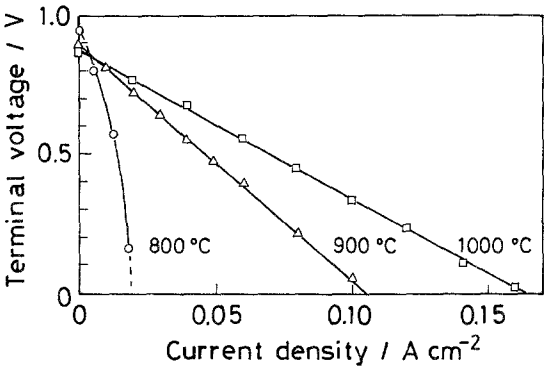

Fig. 7. Discharge curves of the fuel cell using wet CO; CO + H_2O, Pt|$SrCe_{0.95}Yb_{0.05}O_{3-\alpha}$|Pt, air ($P_{H_2O}$ is 23.8 torr in both gases).

900° C (Fig. 7). When dry argon was passed through the cathode compartment instead of air, hydrogen could be electrochemically extracted on sending direct current to the cell. Detailed studies on hydrogen extraction from wet CO will be presented elsewhere.

Finally, ethanol vapour was used as a fuel. Argon gas saturated with aqueous ethanol (1 : 1) at room temperature was introduced to the anode compartment. In this case, hydrogen was produced by the thermal decomposition of ethanol. The e.m.f. of the cell was about 900 mV at 800 to 900° C and a steady and stable current could be drawn (Fig. 8). In the exhaust gas from the anode, H_2, CO and trace amounts of C_2H_4 were observed.

The major limitation of these cells using wet CO or C_2H_5OH as the fuel was also the resistance of the solid electrolyte. Besides such ohmic loss, the cathodic polarization was dominant, while the polarization was negligible at the anode in both cells, similar to our observation in previous cells.

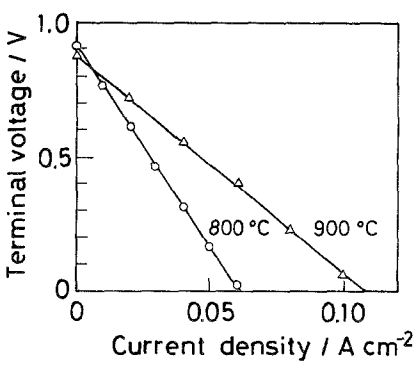

Fig. 8. Discharge curves of the fuel cell using ethanol vapour; C_2H_5OH + H_2O(Ar), Pt|$SrCe_{0.95}Yb_{0.05}O_{3-\alpha}$|Pt, air ($P_{C_2H_5OH}$ = 21.8 torr, P_{H_2O} in fuel gas = 14.6 torr, P_{H_2O} in air = 17.5 torr).

4. Conclusion

Using the high temperature-type proton conductive solid electrolyte based on $SrCeO_3$ various types of fuel cells could be constructed. Not only hydrogen but also different kinds of gases which liberate hydrogen at high temperature could be utilized as the fuel for the cell.

When ethane was used as a fuel, the proton conductor cell generated both electric power and ethylene as a by-product. On passing direct current to this cell, pure hydrogen could be electrochemically extracted from the pyrolysed gas of ethane.

The major limitation of these cell systems using various fuels was the high resistance of the solid electrolyte. Such cell devices with proton conductors may be applied in the simultaneous generator of electricity and ethylene from hydrocarbons, especially if the electrolyte can be used as a thin film in order to reduce ohmic loss.

Acknowledgement

We would like to thank the Ministry of Education, Science and Culture of Japan for supporting part of this work by a grant from the Special Research Project on the Effective Use of Energy (320).

References

[1] F. J. Rohr, 'Applications of Solid Electrolytes (edited by T. Takahashi and A. Kozawa), JEC Press, Cleveland (1980) p. 196.
[2] S. V. Kaparachov, A. T. Filyayev and S. F. Palgayev, *Electrochim. Acta* **9** (1964) 1681.
[3] T. Takahashi, K. Ito and H. Iwahara, *ibid.* **12** (1967) 21.
[4] C. S. Tedmon Jr, H. S. Spacil and S. P. Mitoff, *J. Electrochem. Soc.* **116** (1969) 1170.
[5] T. Takahashi, H. Iwahara and I. Ito, *Denki Kagaku* **38** (1970) 288.
[6] *Idem, ibid.* **38** (1970) 509.
[7] T. H. Etsell and S. N. Flengas, *J. Electrochem. Soc.* **118** (1971) 1980.
[8] R. D. Farr and C. G. Vayenas, *ibid.* **127** (1980) 1478.
[9] A. O. Isenberg, *Solid State Ionics* **3/4** (1981) 431.

[10] Y. Ohno, S. Nagata and H. Sato, *ibid.* **3/4** (1981) 439.
[11] A. Negishi, K. Nozaki and T. Ozawa, *ibid.* **3/4** (1981) 443.
[12] B. G. Ong, C. C. Chiang and D. M. Mason, *ibid.* **3/4** (1981) 447.
[13] D. C. Fee and J. P. Ackerman, US DOE Report, [CONF-831104–1] (1983).
[14] D. C. Fee, S. A. Zwick and J. P. Ackerman, US DOE Report, [CONF-8308120–1] (1983).
[15] G. R. Fitterer, US DOE Report, [DOE/IR/10264–T1] (1980).
[16] T. Takahashi and H. Iwahara, *Energy Conversion* **11** (1971) 105.
[17] D. S. Tannhauser, *J. Electrochem. Soc.* **125** (1978) 1277.
[18] H. Iwahara, T. Esaka, H. Uchida and N. Maeda, *Solid State Ionics* **3/4** (1981) 359.
[19] H. Iwahara, H. Uchida and T. Esaka, *Prog. Batteries Solar Cells* **4** (1982) 279.
[20] H. Iwahara, H. Uchida and N. Maeda, *J. Power Sources* **7** (1982) 293.
[21] H. Iwahara, H. Uchida and S. Tanaka, *Solid State Ionics* **9/10** (1983) 1021.
[22] H. Uchida, S. Tanaka and H. Iwahara, *J. Appl. Electrochem.* **15** (1985) 93.
[23] H. Uchida, N. Maeda and H. Iwahara, *ibid.* **12** (1982) 645.
[24] H. Iwahara, H. Uchida and J. Kondo, *ibid.* **13** (1983) 365.
[25] H. Iwahara, H. Uchida and N. Maeda, *Solid State Ionics* **11** (1983) 109.
[26] R. Tsou, *Sci. Sin.* **22** (1979) 53.
[27] W. M. Lee and C. T. Yeh, *J. Phys. Chem.* **83** (1979) 771.
[28] G. Pratt and D. Rogers, *J. Chem. Soc. Faraday Trans.* **75** (1979) 1089.
[29] M. Stoukides and C. G. Vayenas, *J. Electrochem. Soc.* **131** (1984) 839.
[30] C. J. West, International Critical Tables, Vol. VII, McGraw-Hill, New York (1930), p. 243.